



## OPEN Land use and land cover classification and terrestrial ecosystem carbon storage changes in Vietnam based on Sentinel images

Yang Liu<sup>1,2</sup>, Kun Yang<sup>1,2</sup>✉, Zongqi Peng<sup>1,2</sup>✉, Tianle Zou<sup>1,2</sup>, Danni Su<sup>1,2</sup>, Run Sun<sup>1,2</sup> & Jingcong Ma<sup>1,2</sup>

As the world's second-largest rice exporter, Vietnam's monitoring of land cover changes and carbon stock estimation is crucial for achieving its carbon neutrality goals amidst deforestation and industrial upgrading. This study developed a new land cover classification method based on the phenological characteristics of rice, using the Google Earth Engine (GEE). The method significantly improves the identification accuracy of farmland by extracting rice phenological bands from Sentinel-1 radar data and Sentinel-2 multispectral data. Carbon stock data from 2015 to 2023 were generated using the InVEST model, and their spatial-temporal variations were analyzed. Additionally, the driving factors behind the changes in carbon stocks in forests, grasslands, and croplands were quantitatively explored using the geographic detector (Geo-Detector). The results show that: (1) The classification method for land cover created in this research exhibits greater accuracy than the European Space Agency (ESA) global land cover map and the Japan Aerospace Exploration Agency (JAXA) forest/non-forest maps from Japan, achieving an overall classification accuracy that surpasses 90%. This method also addresses the issue of low identification accuracy of croplands in traditional methods. (2) From 2015 to 2023, Vietnam's LULC changes were mainly characterized by decreases in forests and croplands, and increases in grasslands, construction land, bare land, and water bodies. (3) Overall, natural factors have a greater influence on LULC distribution in Vietnam than human activities, with slope being the most influential factor, followed by altitude, temperature, and population. (4) The main factors affecting the reduction of forest and cropland areas were slope, altitude, and population, while the main factors influencing the changes in construction land area were population and the economy. (5) Vietnam's average carbon stock from 2015 to 2023 was 2.312 billion tons, with an average annual change rate of  $-0.63\%$ . Accurate identification of land cover types is a prerequisite for precise carbon stock estimation, and accurate carbon stock estimates are crucial for advancing Vietnam's carbon neutrality goals.

Effective strategies to combat rising global average temperatures include reducing carbon dioxide (CO<sub>2</sub>) emissions and enhancing the efficiency of CO<sub>2</sub> uptake by terrestrial ecosystems<sup>1</sup>. Land ecosystems act as important carbon stores in the carbon cycle, contributing significantly to the mitigation of global climate change and the attainment of regional carbon neutrality objectives. Modifications in land use and land cover (LULC) represent a major way in which ecosystems have been transformed by human activities<sup>2</sup>. LULC are also major carriers that contribute to carbon emissions<sup>3</sup>. Studies have shown that tropical regions worldwide exhibit trends of cropland expansion, agricultural intensification, pasture expansion, tropical deforestation, and urban growth<sup>4</sup>. These trends are driven by factors such as climate, policies, and economic development. As a tropical country, Vietnam has experienced rapid economic development since joining the World Trade Organization, which has made these LULC changes even more pronounced. Moreover, LULC changes affect terrestrial ecosystem carbon storage by altering ecosystem structure. In terrestrial ecosystems, vegetation recovery, forest regeneration,

<sup>1</sup>Faculty of Geography, Yunnan Normal University, Kunming 650500, China. <sup>2</sup>The Engineering Research Centre of GIS Technology in Western China, Ministry of Education of China, Yunnan Normal University, Kunming, China. ✉email: kmdcynu@163.com; pengzongqiynnu@163.com

and wetland conservation have positive effects by increasing carbon storage, whereas deforestation, forest degradation, grassland conversion, and the expansion of bare land have negative effects by reducing carbon storage<sup>5</sup>. Therefore, in the context of gradual environmental changes in terrestrial ecosystems globally, Precise and logical observation of LULC changes, along with the assessment of carbon reserves in terrestrial ecosystems, is crucial for attaining carbon neutrality<sup>6</sup>. A number of initiatives have been implemented in countries around the globe to achieve the goal of carbon neutrality<sup>7</sup>. Where optimizing LULC is an important way to do this at the foundation level and is an important part of the natural foundation solution<sup>8,9</sup>. It is essential to analyze the changes in LULC associated with changes in carbon stocks, which can lead to the timely identification of problems in the past LULC development process and provide an important reference for LULC management<sup>2</sup>.

Recently, there has been considerable interest in research that investigates the effects of changes in LULC on carbon storage within terrestrial ecosystems<sup>10,11</sup>. Accurate LULC changes respond to human-environment interactions<sup>12</sup>. In the method of classifying LULC, the enhancement of classification outcomes is greatly affected by both spectral properties and textural features<sup>13</sup> by integrating diverse datasets, which encompass optical and radar satellite images<sup>13,14</sup>. Prior research has sought to combine various forms of remote sensing data and leverage their distinct features for the production of precise LULC maps. The Sentinel-1 (S1) data provide complementary information to the optical Sentinel-2 (S2) data, so LULC classification can improve classification accuracy by integrating these two data sources. Phenological features can improve classification accuracy by capturing seasonal variations, reducing the mixed pixel problem, and providing additional discriminative features. In this experiment's LULC classification task, we further enhanced the classification results by incorporating regional vegetation phenological features. The advancement of satellite remote sensing information<sup>14</sup> the establishment of the GEE cloud computing system<sup>15</sup> the implementation of methods based on time series<sup>16</sup> and the utilization of machine learning techniques along with deep learning approaches<sup>13,17</sup> have brought new perspectives to the field of large-scale LULC mapping. Random forests have been used on a large scale for remote sensing map classification because of their fast computing speed and high data processing efficiency<sup>15</sup>. Cloud computing platform, GEE, provides high computational power and easy access to dense time series<sup>18</sup>. GEE also provides a wealth of satellite data and remote sensing-derived products<sup>19</sup>. By utilizing the GEE platform, users can eliminate the need for local image storage and access enhanced computing resources for image analysis and processing<sup>20</sup>. The Geo-Detector method, as a quantitative approach for analyzing spatial distribution differences and their driving factors, is widely used to compare the relationships between various influencing factors and LULC<sup>21</sup>.

There are various methods for estimating carbon storage, with traditional methods including sample inventories<sup>22</sup> field surveys, biomass methods, and ecosystem carbon flux monitoring<sup>23</sup>. Assessment models such as CASA<sup>24</sup>. Book keeping<sup>25</sup> and Integrated Valuation of Ecosystem Services and Trade-offs (InVEST)<sup>26</sup> are commonly used. Traditional estimation methods are labor-intensive and inefficient, making them suitable only for small-scale carbon storage studies. In contrast, the use of the InVEST model for carbon storage estimation based on LULC classification maps effectively illustrates the relationship between long-term time series data and significant carbon storage changes caused by natural events and human activities. Among many assessment models, the InVEST model is widely applied in carbon storage estimation across various countries and regions due to its small data requirements, fast computation speed, and ability to achieve spatiotemporal visualization<sup>27,28</sup>. In this study, the data required for carbon storage estimation is the LULC classification map. While this method can assess and visualize changes in carbon storage across different scales, it also has limitations, such as focusing on a single carbon pool with weak comprehensive analysis capabilities, relying on medium to low-resolution LULC data that struggles to accurately capture small-scale LULC changes, and only being able to assess the carbon storage distribution at a single point in time, without monitoring long-term dynamic changes in carbon storage<sup>29</sup>.

As the second largest rice exporter in the world<sup>30</sup> there are still relatively few LULC studies on Vietnam. Vietnam has 7.66 million hectares of rice farmland, and this study fully integrates this geographical feature in LULC classification. Extracts the second season (summer and autumn) rice phenology characteristics among the three seasons of rice through several comparative experiments, and realizes a large area of Vietnam through the GEE cloud platform in combination with the S1 and S2 data while the classification accuracy is further improved to monitoring. Providing support for thereby realizing sustainable industrial development in Vietnam in the context of carbon neutrality. As a major rice-producing country, Vietnam has vast areas of irrigated rice fields. These rice fields exhibit distinct phenological characteristics during the rice-growing season. Extracting these phenological features can help improve the accuracy of LULC classification in the region<sup>31</sup>.

This study utilized 10-meter resolution Sentinel-1 (S1) and Sentinel-2 (S2) data to generate Vietnam's LULC classification map, providing a foundation for subsequent analyses. Using the Geo-Detector model, we examined the influence of various natural and social factors on LULC. Additionally, LULC changes across different regions of Vietnam were encoded using the Raster Calculator, enabling a better understanding of LULC transitions, particularly the shift from mountainous forests to coastal plains. This analysis contributes to a deeper understanding of the relationship between LULC changes and carbon storage. In this study, data on LULC and carbon density are integrated to assess carbon stocks in Vietnam from 2015 to 2023 using the InVEST model, with the aim of creating a carbon stock map. A quantitative analysis is conducted to further investigate how natural and socio-economic factors influence changes in LULC and their effect on carbon stock. The results of the study contribute to the development of effective strategies for carbon management and methods for forest conservation that seek to enhance sustainable development in the region.

## Methodology

### Study area

Vietnam shares its northern border with China, is adjacent to Laos and Cambodia to the west, and confronts the South China Sea to the east and south, encompassing an area of  $33.1 \times 10^4 \text{ km}^2$  (Fig. 1). The landscape varies

greatly, consisting of rugged mountains in the northern region and extensive river deltas towards the south. The north is mountainous, including the Himalayas. The central part of the country is hilly and low mountainous, an important agro-industrial base with a rich ecosystem. The southern Mekong River Delta is characterized by a tropical monsoon climate with high temperatures throughout the year and distinct dry and rainy seasons. The annual average rainfall ranges from 1500 to 2000 millimeters. The region features fertile soil and low-lying terrain, making it well-suited for agricultural production. The northern area of the country experiences four unique seasons, whereas the south-central region is subjected to a tropical monsoon climate, noted for its high temperatures and humidity throughout the year, averaging an annual temperature of 24 °C. With a population of 97.58 million individuals across 58 provinces and 5 municipalities, Vietnam boasts a diverse food production system, highlighted by its significant rice output, positioning the country as the world's second-largest rice exporter. Since joining the World Trade Organization (WTO) in 2007, Vietnam has experienced rapid economic development, gradually transitioning from an agricultural country to a producer and exporter of electronic products in the global industrial supply chain. Studies have shown that economic growth is closely associated with increased carbon dioxide emissions. Consequently, Vietnam faces significant carbon emissions from its economic activities, while also holding substantial potential for reducing these emissions. This is critical for achieving carbon neutrality goals in Southeast Asia. Therefore, studying Vietnam's carbon storage in recent years has become an urgent and pressing task.

### Data sources and preprocessing

Tables 1 and 2 constitute the primary data sources for this study, including S1 and S2 satellite data, as well as natural and socio-economic factors that may influence land cover changes (Table 1). Among them, natural factors emphasize those unrelated to human activities. S1 provides synthetic aperture radar (SAR) imagery, which is primarily used to obtain structural and moisture information on the ground surface, whereas S2 imagery is capable of capturing more detailed information about surface vegetation and other features. Two types of image data are essential for accurately analyzing LULC classifications in Vietnam. To ensure the precision of LULC classification, a resolution of 10 m was determined at this phase. Based on previous studies<sup>32,33</sup> we identified seven socio-economic and natural factor indicators as the main factors influencing LULC change.

In the first stage of processing S1 and S2 remote sensing data, a Class 1 ground probe scene was selected that includes the vertical-vertical (VV) and vertical-horizontal (VH) bands from the S1 dataset, which operates in an interferometric wide (IW) stripe mode in either an “ascending” or “descending” orbit. To effectively depict the backscatter from the surface, the SAR data requires pre-processing steps such as the removal of thermal noise, radiometric calibration, and terrain adjustment. This is essential for subsequent LULC classification<sup>34</sup>. To reduce the impact of speckle noise and shadows, we used the annual average values of VV and VH in subsequent calculations. For the S2 data, we performed an atmospheric correction to convert the top-of-atmosphere reflectance data to ground reflectance to minimize the effects of atmospheric scattering and absorption<sup>35</sup>. In the following research, we exclusively employed the blue, green, red, and near-infrared (NIR) bands with a spatial resolution of 10 m, alongside the narrow NIR, red-edge 1–3, and short-wave infrared (SWIR) 1–2 bands at a spatial resolution of 20 m. These bands are identified as B2, B3, B4, B5, B6, B7, B8, B8A, B11, and B12 (Table 3), correspondingly. At the same time, considering that the abundant rainfall and cloud cover in Vietnam may lead to a data quality degradation, a cloud coverage screening algorithm was used in order to obtain images with low cloud coverage (<40% cloud). In addition, we used the quality assessment (QA60) band to avoid cloud-contaminated pixels. In order to maintain both temporal and spatial consistency in the data, we applied a median annual synthesis method to the images, which removes extreme values such as extremely bright or dark pixels due to the sensor during the imaging process by selecting the median reflectance of each pixel point over the course of the year<sup>36</sup>.

Three spectral indices were computed to improve the distinction between vegetation, developed areas, and water bodies within the main LULC categories in Vietnam: the Normalized Difference Vegetation Index (NDVI), the Normalized Difference Built-up Index (NDBI), and the Modified Normalized Difference Water bodies Index (MNDWI). The calculations for these indices are illustrated by Eqs. 1–3:

$$NDVI = \frac{NIR - Red}{NIR + Red} \quad (1)$$

$$NDBI = \frac{SWIRI - NIR}{SWIRI + NIR} \quad (2)$$

$$mNDVI = \frac{Green - SWIRI}{Green + SWIRI} \quad (3)$$

In this study, we collected time series images of the VV and VH bands throughout the rice growing season from the S1 radar data to extract indicators reflecting the climatic characteristics of rice for each year. We computed five texture variables from the VV and VH images annually by employing a gray-scale covariance matrix. This matrix incorporates angular second-order moments (ASM), entropy (ENT), inverse differential moments (IDM), correlation (CORR), and the average summed value (SAVG). These variables effectively capture texture features related to LULC<sup>37</sup>. The extracted features were used alongside the annual composite optical and backscatter bands as inputs to the classifier (Table 2). The matrix calculation formula is as follows:

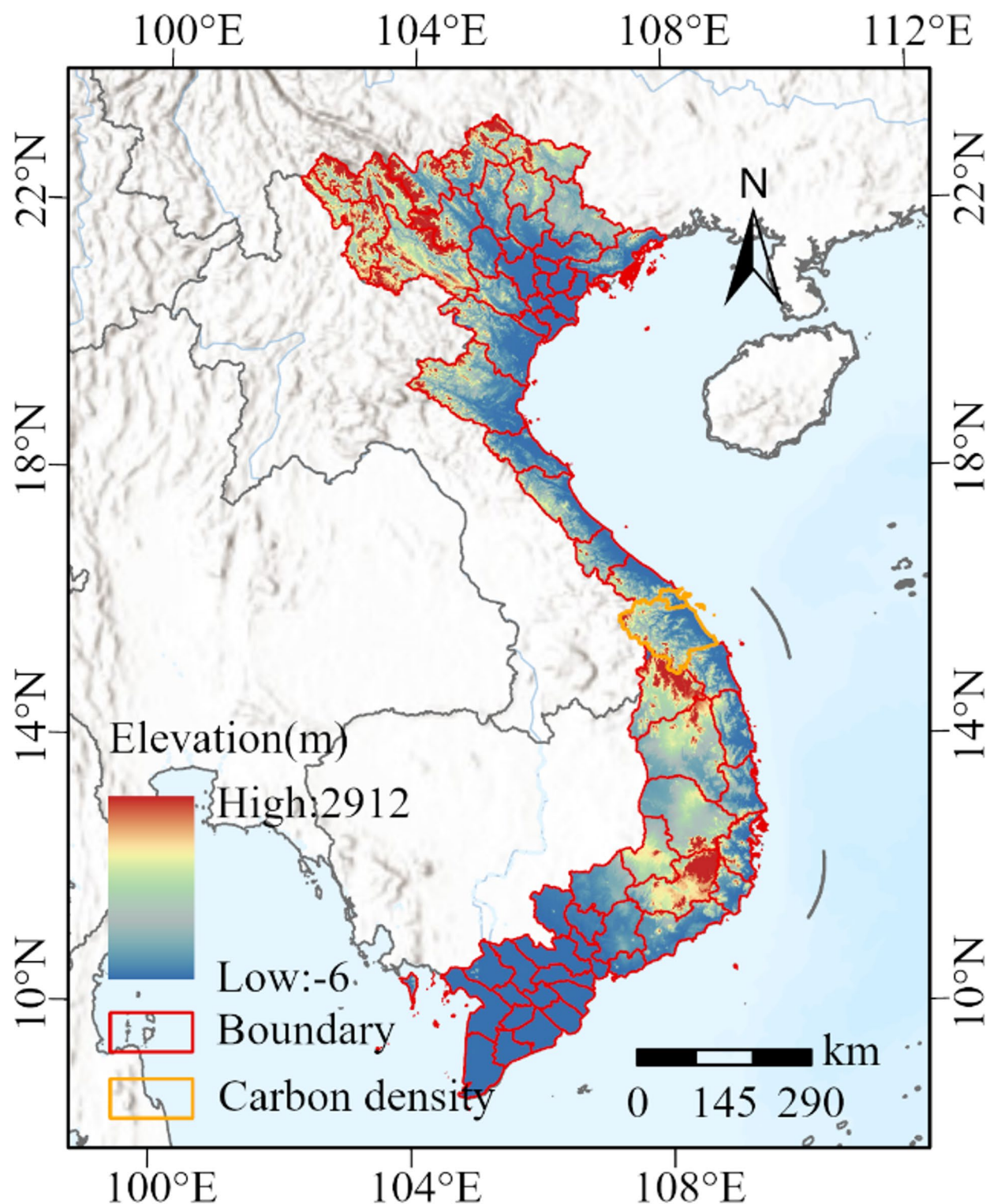


**Fig. 1.** Location of the study area. This figure is generated using ArcGIS Pro 3.0.1 (<https://www.esri.com/zh-cn/arcgis/products/arcgis-pro/overview>), with the base maps sourced from the World\_Hillshade ([https://goto.arcgisonline.com/maps/Elevation/World\\_Hillshade](https://goto.arcgisonline.com/maps/Elevation/World_Hillshade)) and World Topographic Map (<https://www.arcgis.com/home/item.html?id=7dc6cea0b1764a1f9af2e679f642f0f5>). The country boundary is extracted from the GADM (<https://gadm.org/>).



Category	Name	Time	Source	Resolution
Natural factors	Elevation	2007	National Aeronautics and Space Administration Jet Propulsion Laboratory ( <a href="https://doi.org/10.1029/2005RG000183">https://doi.org/10.1029/2005RG000183</a> )	90 m
	Slope	2007	National Aeronautics and Space Administration Jet Propulsion Laboratory ( <a href="https://doi.org/10.1029/2005RG000183">https://doi.org/10.1029/2005RG000183</a> )	90 m
	Aspect	2007	National Aeronautics and Space Administration Jet Propulsion Laboratory ( <a href="https://doi.org/10.1029/2005RG000183">https://doi.org/10.1029/2005RG000183</a> )	90 m
	Temperature	2015–2020	Climate Data Store( <a href="https://cds.climate.copernicus.eu">cds.climate.copernicus.eu</a> )	31 km
	Precipitation	2015–2020	Climate Hazards Center( <a href="https://chc.ucs.edu">https://chc.ucs.edu</a> )	5 km
Socioeconomic factors	Population	2015–2020	WorldPop( <a href="http://www.worldpop.org">www.worldpop.org</a> )	100 m
	GDP	2015–2020	( <a href="https://doi.org/10.6084/m9.figshare.17004523.v1">https://doi.org/10.6084/m9.figshare.17004523.v1</a> )	1 km
Boundary	–	–	<a href="https://gadm.org/">https://gadm.org/</a>	–
Basemap	World_Hillshade	–	<a href="https://goto.arcgisonline.com/maps/Elevation/World_Hillshade">https://goto.arcgisonline.com/maps/Elevation/World_Hillshade</a>	–
	World TopographicMap	–	<a href="https://www.arcgis.com/home/item.html?id=7dc6cea0b1764a1f9af2e679f642f0f5">https://www.arcgis.com/home/item.html?id=7dc6cea0b1764a1f9af2e679f642f0f5</a>	–

**Table 1.** Data sources.

Data source	Input features	Dimension
S2 MSI	Spectral features: median composition of B2, B3, B4, B5, B6, B7, B8, B8A, B11, B12	10
	Normalized indices: NDVI, NDBI, MNDWI	3
S1 SAR	Backscattering features: annual mean of VV, VH time-series images	2
	Phenological features: may average value of VV, VH band time series images	2
	Temporal features: standard deviation of VH, VV	2
	Textural features: ASM, ENT, IDM, CORR, SAVG of each annual mean of VV and VH	10

**Table 2.** Sentinel 1 & 2 bands considered for the study.

Name	Pixel size (m)	Wavelength range (nm)	Description
B2	10	492.1–496.6	Blue
B3	10	559–560	Green
B4	10	664.5–665	Red
B5	20	703.8–703.9	Red Edge 1
B6	20	739.1–740.2	Red Edge 2
B7	20	779.7–782.5	Red Edge 3
B8	10	833–835.1	NIR
B8A	20	864–864.8	Red Edge 4
B11	20	1610.4–1613.7	SWIR 1
B12	20	2185.7–2202.4	SWIR 2

**Table 3.** Sentinel 2 bands and description.

$$ASM = \sum_{i=1}^N \sum_{j=1}^N P(i, j)^2 \quad (4)$$

$$ENT = - \sum_{i=1}^N \sum_{j=1}^N P(i, j) \cdot \log(P(i, j)) \quad (5)$$

$$IDM = \sum_{i=1}^N \sum_{j=1}^N \frac{P(i, j)}{1 + (i - j)^2} \quad (6)$$

$$CORR = \sum_{i=1}^N \sum_{j=1}^N \frac{(i - \mu_i)(j - \mu_j)P(i, j)}{\sigma_i \sigma_j} \quad (7)$$

$$SAVG = \sum_{i=2}^{2N} i \cdot P_x(i) \tag{8}$$

Where:  $N$  is the total number of gray levels;  $i, j$  are the gray values, and  $P(i, j)$  is the normalized value of the gray-level co-occurrence matrix (GLCM);  $\mu_i$  is the mean of gray level  $i$ , calculated as:  $\mu_i = \sum_{j=1}^N i \cdot P(i, j)$ ;  $\sigma_i$  is the standard deviation of gray level  $i$ , calculated as  $\sigma_i = \sqrt{\sum_{j=1}^N (i - \mu_i)^2 \cdot P(i, j)}$ ;  $P_x(i)$  is the joint probability distribution function of the gray-level co-occurrence matrix.

The carbon storage density data presented in this study originates from the Vu Gia Thu Bon River Basin in central Vietnam. It was calculated by Valerio Avitabile and his colleagues using a stratified random sampling design. The data was derived from field measurements of forest inventory plots to estimate the carbon storage density of aboveground biomass. Meanwhile, the estimation for the carbon stock density of below-ground biomass was informed by the average root-crown ratio (R) recommended by the IPCC<sup>29</sup>. The assessment was conducted within the specified study area. Relevant data are shown in Table 4. Due to the large geographic span and diverse forest types across Vietnam, it is difficult to accurately estimate the carbon storage of forests with varying densities and tree species. However, in a forest, the density tends to gradually increase from the forest edge to the forest center. Therefore, in this study, the calculation of all forest carbon storage was based on biomass data from forests with medium density.

Random forest classification based on sentinel images

In this research, the random forest algorithm serves as the machine learning technique employed for predicting LULC. This approach is a form of integrated learning that enhances classification accuracy and stability by building several decision trees and combining their outcomes<sup>38</sup>. Here, we examined time series data from S1 and S2 through the random forest method to discern and categorize the primary LULC types in Vietnam, which encompass forests, grasslands, agricultural areas, developed lands, barren land, and water bodies, utilizing the overall accuracy (OA) as a measure of classification performance. In this study, we found that S1 imagery collection began on June 27, 2015, resulting in less than a full year of S2 imagery coverage for Vietnam in 2015. More importantly, due to climatic conditions, it was challenging to find low-cloud-cover imagery for Vietnam in 2015. To enhance the reliability of the experiment, we used only S1 imagery to extract the LULC classification map for 2015. A similar situation occurred in 2016 for six provinces in northern Vietnam: Yen Bai, Lao Cai, Ha Giang, Tuyen Quang, Son La, and Phu Tho. These provinces experienced persistent cloud cover, making it difficult to obtain low-cloud-cover imagery. Consequently, we adopted a similar approach to extract the LULC maps for these regions in 2016.

To train the Random Forest model, we first randomly selected 6000 sample points within Vietnam using a random sampling method. We extracted the LULC types of these sample points from existing LULC classification datasets, which include: (1) The ESA World Cover 2020 (resolution: 10 m, time: 2020); (2) The ESA World Cover 2021 (resolution: 10 m, time: 2021); (3) The Global Forest/Non-Forest Map (FNF) (resolution: 25 m, time: 2017–2021); (4) The Copernicus Global Land Service Dynamic LULC map (CGLS-LC100) (resolution: 100 m, time: 2015–2019); (5) GHSL: Global Settlement Characteristics (GHSL) (resolution: 10 m, time: 2018). We retained sample points with the same LULC type and removed those with differing types, resulting in 5000 multi-year stable sample points. Subsequently, we randomly selected an additional 1000 sample points within Vietnam and annotated their LULC types for each year using a visual interpretation method to supplement the stable sample points.

In GEE, the model training was configured with 500 decision trees, optimizing efficiency and classification accuracy by using the square root of the number of variables required for splitting each tree node. For input features, we included basic spectral bands, spectral index bands, radar bands, texture variable bands, and synthesized phenological feature bands extracted during the rice-growing season. This combination of features enhanced the classification accuracy in the LULC task. A 3 × 3 median filter was applied to the classification results to reduce potential salt-and-pepper noise and ensure more accurate and reliable LULC change results.

The integration of spectral, texture, and phenological features not only improved LULC classification accuracy but also laid a solid foundation for future carbon storage assessments. During the Random Forest classification process, we calculated the contribution rates of different bands and selected bands with contribution rates between 415 and 655 as reference bands for classification. The relevant data are summarized in Table 5.

Land cover class	Carbon stock (Mg C/ha)			Source
	AGB	BGB	AGB + BGB	
Forest rich	166.8	39.2	206	Field data
Forest medium	83	19.5	102.5	Field data
Forest poor	44.5	9.1	53.6	Field data
Grassland	6.5	1.3	7.9	Field data
Cropland	4	1	5	IPCC tier 1

Table 4. Carbon density data.

Mapping of LULC changes

LULC mapping can track in detail the process of LULC type transformation from one state to another in a specific area, such as the transformation to farmland after deforestation or the reduction of forest due to urban expansion. This study employs a raster calculator to analyze high-resolution LULC data from 2015, 2019, and 2023. LULC types are encoded with corresponding numerical values, which are weighted and summed to generate LULC maps for 2015–2019 and 2019–2023. Through numerical analysis of these maps, the spatial distribution and quantity of mutual transformations between different LULC types during these periods can be determined. The specific steps are as follows: (1). Assign numerical codes (1, 2, 3, ..., 6) to six LULC types: forest, grassland, farmland, built-up land, bare land, and water bodies, respectively. (2). Weight the numerical codes of the starting date by a factor of 10. (3). Add the weighted numerical codes of the starting date directly to the numerical codes of the ending date to create LULC maps. The formula is expressed as shown in Eq. 9:

$$L = (Y_1) \times 10 + (Y_2) \tag{9}$$

Where  $L$  represents the synthesized LULC code,  $Y_1$  denotes the LULC code at the starting date, and  $Y_2$  denotes the LULC code at the ending date. The mapping codes are progressively aggregated over the relevant period to generate a LULC change map and a spatiotemporal evolution map, illustrating the patterns of LULC transformation during this period.

InVEST model

The InVEST model is an open-source software tool for assessing and quantifying ecosystem services. This model supports carbon storage estimation services. Through this model, we can achieve the conversion from aboveground and belowground biomass to carbon storage. The calculation principle is shown in Eq. 10:

$$C_i = A_i \times (C_{agb} + C_{bgb} + C_{soc} + C_{dom}) \tag{10}$$

Where:  $C_i$  represents the total carbon storage of LULC type  $i$ ;  $A_i$  represents the area of LULC type  $i$ ;  $C_{agb}$  represents the aboveground biomass carbon pool, typically referring to the carbon stored in the aboveground parts of plants such as trees, grasslands, and crops;  $C_{bgb}$  represents the belowground biomass carbon pool, usually referring to the carbon stored in plant root systems;  $C_{soc}$  represents the soil organic carbon pool, typically referring to the organic carbon storage in the soil, which varies with LULC types and soil depth;  $C_{dom}$  represents the litter carbon pool, generally referring to the carbon stored in fallen leaves, deadwood, and other detritus within a region.

In this study, we used LULC classification map data for Vietnam obtained through GEE and the measured carbon storage data from the Vu Gia Thu Bon River Basin in central Vietnam (Table 4) as input data. Using the InVEST model, we calculated the annual carbon storage summary tables and carbon storage raster maps for each year.

Geo-detector model

The Geo-detector method is a statistical technique used to explore influencing factors. It detects spatial dissimilarity by considering and quantifying the non-linear relationships, scale effects and interactions between spatial factors, and combines q-statistical theories with objective and quantitative hierarchical analyses of geographic features, which are more widely used in revealing the intrinsic laws and mechanisms behind geographic phenomena, with the model principles as follows. The Geo-detector was implemented using the Excel Geo-Detector software created by Wang et al.<sup>39</sup> which is available for free at the website (<http://www.ge>

Name	Contribution rate	Name	Contribution rate
NDVI	652	VV_ent	535
B4	647	Y_VH	531
MNDWI	640	VV_savg	521
B5	627	B11	519
B3	607	VH_idm	518
VH_savg	607	VV_asm	514
VH_Phenological characteristics	595	B6	480
B12	580	B7	471
NDBI	577	B8A	470
B2	549	VH_asm	470
VV_idm	548	B8	456
VV_Phenological characteristics	546	VH_corr	456
VH_stdDev	542	VH_ent	428
VV_stdDev	541	VV_corr	419
VV	535		

Table 5. Parameter’s contribution rate as observed in random forest classification.

odetector.cn). This factor detector assesses how much each factor explains the spatial variability in vegetation phenology. A higher q value indicates greater explanatory strength of the factor regarding climate, as quantified by the q value, with its formulation presented in Eqs. 11 and 12:

$$q = 1 - \frac{\sum_{h=1}^L N_h \sigma_h^2}{N \sigma^2} = 1 - \frac{SSW}{SST} \tag{11}$$

where:  $SSW = \sum_{h=1}^L N_h \sigma_h^2$  (sum of squares within groups); (total sum of squares);  $N_h$  is the number of samples in group  $h$ ;  $\sigma_h^2$  is the variance of group  $h$ ;  $N$  is the total number of samples, and  $\sigma^2$  is the total variance.

The interaction detector identified the interactions between environmental factors and evaluated how strongly these interactions explained variations in the dependent variable Y. By analyzing the q-value of an individual factor alongside the combined q-values of two factors and the q-value resulting from their interaction, the study assessed whether the interactions between factors had a strengthening or diminishing effect on vegetation phenology<sup>39</sup>.

**Results**  
**Comparison of accuracy of LULC classification datasets**

Upon completing the classification process, we compared the accuracy of the classification outcomes from the land classification model developed in this research with the global Class 4 PALSAR-2/PALSAR forest/non-forest maps produced by the JAXA (25 m resolution) and the World Cover 10 m v100 maps generated by ESA (10 m resolution). The results of this comparison are presented in Table 6. For the evaluation, this study selected 100 sample points for each LULC type using a visual interpretation method, covering the six land classes identified in this research. The land classes corresponding to these sample points were then extracted from the forest/non-forest maps, the ESA global LULC maps, and the classification result maps generated in this study using GEE.

In this study, the combination of rice growth cycle climate information effectively improves the accuracy of cropland extraction, and at the same time, the regional sample points used in this paper have better results in LULC classification in Vietnam compared to the global sample points. The accuracies of farmland, build-up land, bare land, and water bodies classification as well as the overall classification results are higher than those of ESA global LULC maps and JAXA forest/non-forest maps, and the overall accuracy is as high as 86.7%, in which forests and water bodies have the highest classification accuracies, followed by constructed land, farmland, and grassland.

**Spatial and temporal changes in LULC**  
**(1) Temporal changes in LULC**

The statistics pertaining to different LULC categories in Vietnam are presented in Table 7. The data for various land area types in Vietnam for the year 2023 reveals that the predominant LULC categories include forests, which encompass a total area of  $22.01 \times 10^{10} m^2$ , representing 66.81% of the overall area. This is followed by farmland, covering  $4.74 \times 10^{10} m^2$  (14.38%), and grasslands at  $3.43 \times 10^{10} m^2$  (10.41%). Other categories include construction land at  $1.37 \times 10^{10} m^2$  (4.15%), water bodies occupying  $1.11 \times 10^{10} m^2$  (3.36%), and bare land, which spans  $0.28 \times 10^{10} m^2$  (0.85%).

Figure 2 presents the LULC map of Vietnam, illustrating a notable rise in the extent of built-up regions and grasslands, along with a reduction in forested and barren areas. Additionally, there has been a steady rise in the area covered by water bodies nationwide from 2015 to 2023, while the area designated for farmland shows slight fluctuations but leans towards stabilization. The area of built-up land changes significantly from 2015 to 2023, growing from  $0.77 \times 10^{10} m^2$  in 2015 to  $1.37 \times 10^{10} m^2$  grassland area increased overall between 2015 and 2020, growing from  $2.74 \times 10^{10} m^2$  to  $4.32 \times 10^{10} m^2$ , and then declined, falling to  $3.34 \times 10^{10} m^2$  in 2023. forested land area declined from  $23.43 \times 10^{10} m^2$  to  $21.51 \times 10^{10} m^2$  and then fluctuated to  $22.01 \times 10^{10} m^2$  in 2023. Bare land area gradually decreased from  $0.56 \times 10^{10} m^2$  in 2015 to  $0.28 \times 10^{10} m^2$  in 2023. The extent of aquatic regions exhibited a pattern of first rising and then falling, with measurements of  $0.84 \times 10^{10} m^2$  in 2015, reaching  $1.53 \times 10^{10} m^2$  in 2018, and subsequently dropping to  $1.11 \times 10^{10} m^2$ . farmland fluctuated less, from  $4.61 \times 10^{10} m^2$  in 2015 to  $4.74 \times 10^{10} m^2$  in 2023.

**(2) Spatial changes in LULC.**

	This study	ESA	JAXA
Index	OA	OA	OA
Forest	1.00	1.00	0.94
Grass	0.65	0.74	0.86
Farm	0.83	0.78	
Build-up	0.93	0.88	
Bare land	0.79	0.70	
Water bodies	1.00	0.96	0.84
Total	0.87	0.84	0.73

**Table 6.** Dataset accuracy comparison.



Type( $\times 10^{10} \text{m}^2$ )	2015	2016	2017	2018	2019	2020	2021	2022	2023
Forest	23.43	22.57	22.19	21.51	21.91	21.5	23.72	22.19	22.01
Grass	2.74	3.88	3.3	4.4	4.19	4.32	3.66	3.44	3.43
Farm	4.61	4.59	5.02	4.38	4.28	4.54	3.67	5.25	4.74
Build-up	0.77	0.65	0.97	0.85	0.87	0.94	0.78	0.91	1.37
Bare land	0.56	0.27	0.35	0.27	0.35	0.32	0.3	0.31	0.28
Water bodies	0.84	0.97	1.12	1.53	1.35	1.32	0.81	0.84	1.11
Total	32.94	32.94	32.94	32.94	32.94	32.94	32.94	32.94	32.94

**Table 7.** LULC area statistics.

The allocation of different LULC categories throughout Vietnam is depicted in Fig. 2. In general, the extent of land utilization within the nation shows considerable spatial variation. Forests are mainly found in the northern and central parts, as well as in the mountainous regions of the south. Conversely, farmland is predominantly found in the lower elevation zones, particularly in the northern Red River Delta and the Mekong Delta. Urban development is primarily focused in cities, with Hanoi and Ho Chi Minh City displaying a notable concentration of built-up land. Areas of bare land are dispersed, chiefly in some developed regions or those experiencing land degradation. The main water bodies include the Red and Mekong Rivers, with extensive aquaculture activities observed in the Mekong Delta located in the south. These features highlight the variations in the natural environment and human activities across different regions of Vietnam.

This research conducts an analysis of LULC changes in Vietnam, examining spatial and temporal aspects every four years (Figs. 3 and 4). Its statistical results (Tables 8 and 9) show that the continuous decrease in forest area is one of the most significant changes in LULC in Vietnam, and this decrease is mainly transformed into grassland, farmland, and land for construction. The decrease in forests is particularly noticeable from 2015 to 2019, while this trend slows down from 2019 to 2023. The primary reason for the expansion of grassland areas is largely due to the transformation of forests and agricultural land, particularly the shift from farmland to grasslands. Conversely, the extent of arable land demonstrates an upward trend followed by a decline, indicating the variable transformations in agricultural land across various phases. Between 2015 and 2019, there was a significant rise in the amount of LULC for farmland; however, the reduction observed from 2019 to 2023 indicates a slow transition of farmland into grassland and other purposes. The continued expansion of built-up land reflects the accelerated urbanization of Vietnam, with particularly significant growth in urban land between 2019 and 2023. The area of bare land increases significantly between 2015 and 2019, but decreases between 2019 and 2023, which may be due to a portion of bare land being repurposed for other land uses or affected by ecological restoration measures. The area of water bodies, on the other hand, is mainly characterized by a transformation with farmland, and between grassland use types.

During the period 2015–2019, the continuous decrease in the area of forests in Vietnam is one of the most significant changes in LULC in Vietnam, and this decrease is mainly transformed into grassland, farmland and built-up land, with 85.03% of forests remaining intact, and the rest being transformed into other land-use types, of which 8.12% is transformed into grassland, 3.79% is transformed into farmland, and 1.56% is transformed into built-up land. By 2019–2023, the area of forests remaining intact has slightly increased to 90.37%. The area of forest converted to grassland and farmland also decreased, to 4.66% and 2.99% respectively. The change in grassland was more significant. During the period 2015–2019, 55.84% of grassland remained intact while 29.45% was converted to forest. The conversion of grassland into farmland, built-up land, bare land and water bodies was 10.57%, 3.42%, 0.3% and 0.39% respectively. By 2019–2023, the area of grassland remaining intact decreases to 46.56%, while the area converted to forest increases significantly to 38.44%. The area of grassland converted to bare land also increases to 1.39%. Farmland showed significant changes in both time periods. During 2015–2019, 68.3% of farmland remained intact while 16.16% was converted to forest and 10.86% to grassland. By 2019–2023, the area of farmland remaining intact increases to 73.74% ha, but the area converted to forest and grassland decreases, to 13.01% and 8.39%. Changes in built-up land are also more significant. Between 2015 and 2019, 63.7% of built-up land remained intact, while 9.32% was converted to forest and 2.91% to grassland. By 2019–2023, there is a significant increase in the area of built-up land remaining in its original state to 80.58%, but there is a decrease in the area converted to forest and grassland, down to 3% and 0.83%, respectively. There is an increase in the area of built-up land converted to bare land, to 2.66%. Bare land remained in its original state during 2015–2019, while 8.89% of bare land was converted to forest and 41.98% to grassland. The transformation of un-farmland into farmland, built-up land, and water bodies accounted for 3.24%, 5.36%, and 4.69%, respectively. By 2019–2023, the area of bare land remaining in its original state decreases to 35.11 and the area converted to forest, farmland and built-up land increases, to 10.91, 15.1 and 13.84%, respectively. Additionally, the portion of bare land transitioned into grassland also saw a decrease, reaching 18.38%. Watersheds showed relatively little change between the two time periods, mainly in terms of conversion to water bodies. Between 2015 and 2019, 92.24% of watersheds remained intact, while 4.4% were converted to farmland. By 2019–2023, the area of watersheds remaining intact decreases to 73.04% and the area converted to farmland increases to 21.99%.

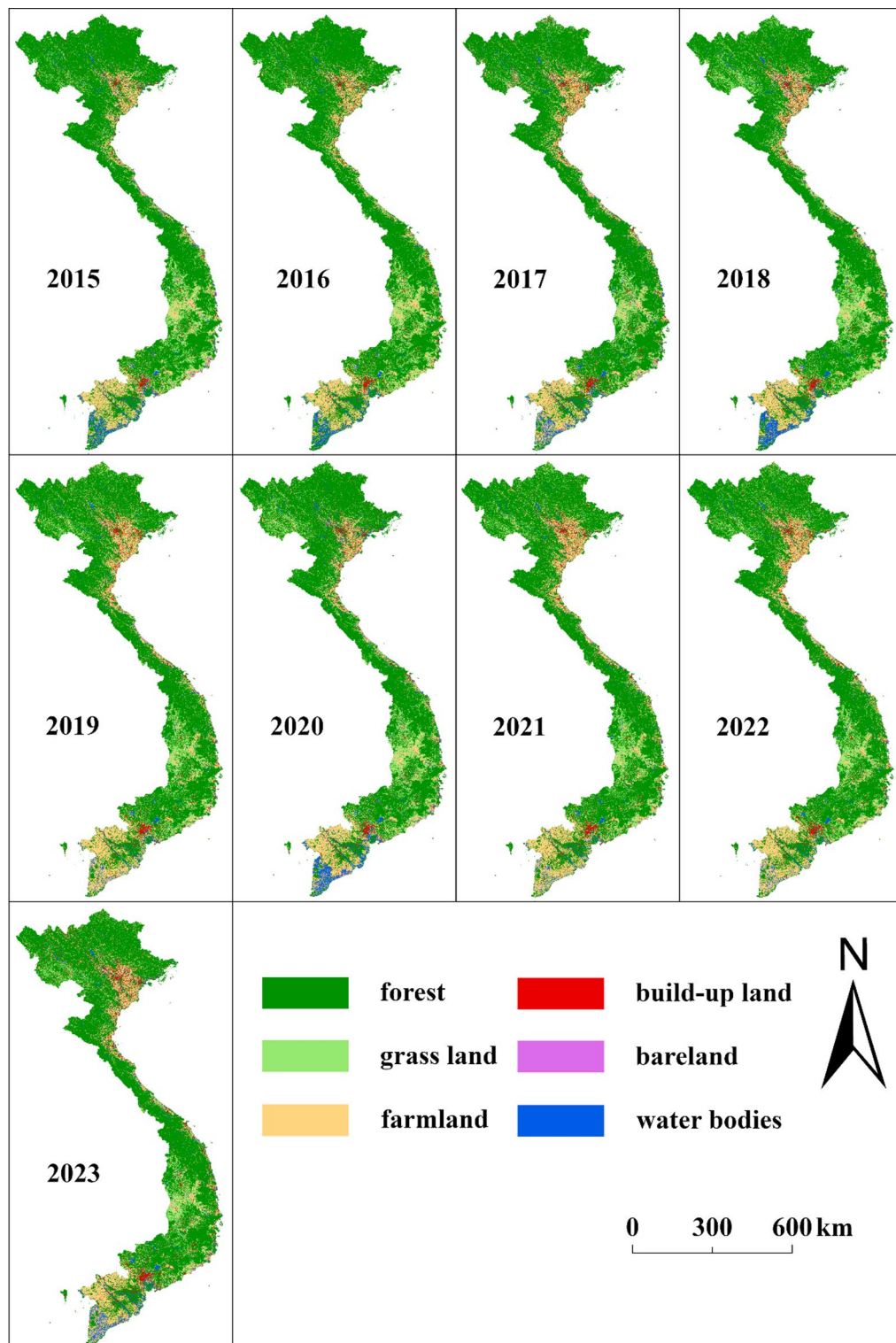


**Fig. 2.** Multi-year LULC maps. This figure is generated using ArcGIS Pro 3.0.1 (<https://www.esri.com/zh-cn/arcgis/products/arcgis-pro/overview>) while the country boundary is extracted from the GADM (<https://gadm.org/>).

### Mechanisms driving LULC change

The interaction heatmap of driving factors based on geographic detection results (Fig. 5) shows that the main influencing factors of forest cover change are slope, elevation, temperature, and population. Among them, slope (0.1819), elevation (0.1707), temperature (0.1245), and population (0.1205) have more significant effects on forest distribution. This indicates that the distribution and changes in forests are influenced by a combination of

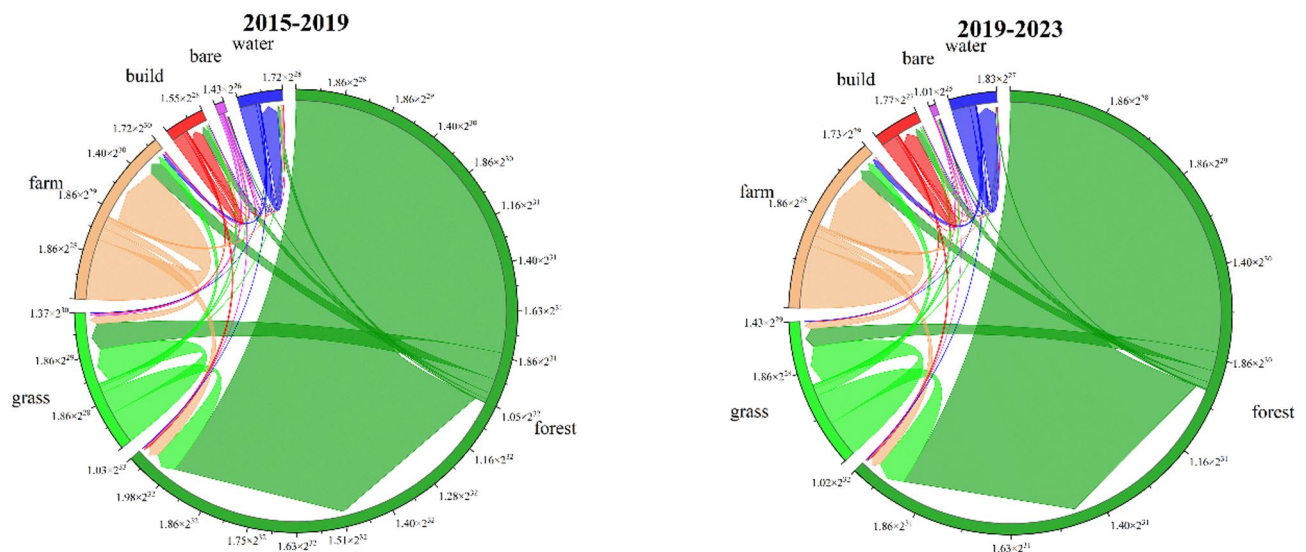


**Fig. 3.** LULC transfer statistics.

topographic conditions as well as climatic factors. In areas with steep slopes, rugged terrain naturally restricts human activities such as agriculture and construction, providing a natural barrier for forest preservation. Meanwhile, regions with moderate altitude and temperature are less likely to be developed by humans and are not constrained by climatic conditions for forest growth, often resulting in higher forest coverage. Influences on grassland distribution are more diffuse, with the effects of elevation (0.0171), slope (0.0177), precipitation (0.0056), temperature (0.0127), and population (0.0037), although less pronounced than those of forests, contributing to the formation of, and changes in, grasslands. Changes in farmland were most influenced by elevation (0.2097), slope (0.1690), temperature (0.1031) and population (0.1287). Due to the low altitude, gentle slopes, abundant water resources, and suitable temperatures in the Red River Delta and Mekong River Delta regions of Vietnam, there has been an expansion of arable land. With the increase in the agricultural population in these areas, the demand for agricultural land has also risen, leading to the conversion of more land into cropland. Changes in built-up land were mainly influenced by population (0.2104) and GDP (0.1048), indicating that construction activities were mainly concentrated in areas with high population density and economic activity. In addition, elevation (0.0350) and slope (0.0209) also have a constraining effect on the distribution of built-up land, as flat and low elevation areas are more suitable for construction and development. The main factors influencing the change of bare land include precipitation (0.0209) and temperature (0.0020), which are climatic factors that have a more significant effect on the distribution of bare land. GDP and population (0.0009) have relatively less influence on bare land, indicating that bare land is more due to natural conditions than human activities. The distribution of water bodies is mainly influenced by elevation (0.0662), slope (0.0368) and temperature (0.0298), which are natural factors that determine the formation and stability of water bodies.

### Characterization of spatial and temporal variations in carbon stocks

In this study, we mapped Vietnam's carbon stock based on the InVEST model (Fig. 7), and combined with the carbon stock statistics (Table 10) and the statistical map of carbon stock changes (Fig. 6), we analyzed the temporal and spatial changes in Vietnam's carbon stock from 2015 to 2023. Overall, as of 2023, Vietnam has  $230.68 \times 10^7 Mg$  of carbon stock. Temporally, the overall carbon stock declines from  $244.59 \times 10^7 Mg$  in 2015 to a low of  $226.04 \times 10^7 Mg$  in 2020, and then gradually rebounds to  $230.68 \times 10^7 Mg$  in 2023. This indicates that between 2015 and 2020 This indicates a decreasing trend in carbon stocks between 2015 and 2020, and a recovery after 2021, with spatially higher carbon stocks in the northern mountainous areas and the central highlands.

In terms of time, forest carbon stocks accounted for the largest share and showed an overall decreasing trend, decreasing from  $240.15 \times 10^7 Mg$  in 2015 to  $220.4 \times 10^7 Mg$  in 2020. it recovered after 2021 and reached  $225.63 \times 10^7 Mg$  in 2023, and the decrease in forest area was one of the main reasons for the decrease in carbon stocks. The overall fluctuation of carbon stock in grassland is larger, increasing from  $2.14 \times 10^7 Mg$  in 2015 to  $3.73 \times 10^7 Mg$  in 2020, and then decreasing, reaching  $2.67 \times 10^7 Mg$  in 2023. The overall fluctuation of carbon stock in farmland has less change, and basically maintains in a more stable range from  $2.3 \times 10^7 Mg$  in 2015, and after 2021 there is a small increase, and in 2023 it is  $2.37 \times 10^7 Mg$ .

Spatially, the distribution of high and low carbon stocks shows clear geographical differences. Mountainous areas in the north of Vietnam (e.g. Ha Giang, Xuan Quang, etc.) show high carbon stocks, the central highlands (e.g. Deloitte, Gia Lai, etc.) also show high carbon stocks, and the Mekong River delta as well as the plains in the south have low carbon stocks. Cities and coastal areas such as Ho Chi Minh City, Da Nang, and Hai Phong generally have low carbon stocks. Coastal areas have low carbon stocks due to high exploitation and reduced vegetation cover (Fig. 7).



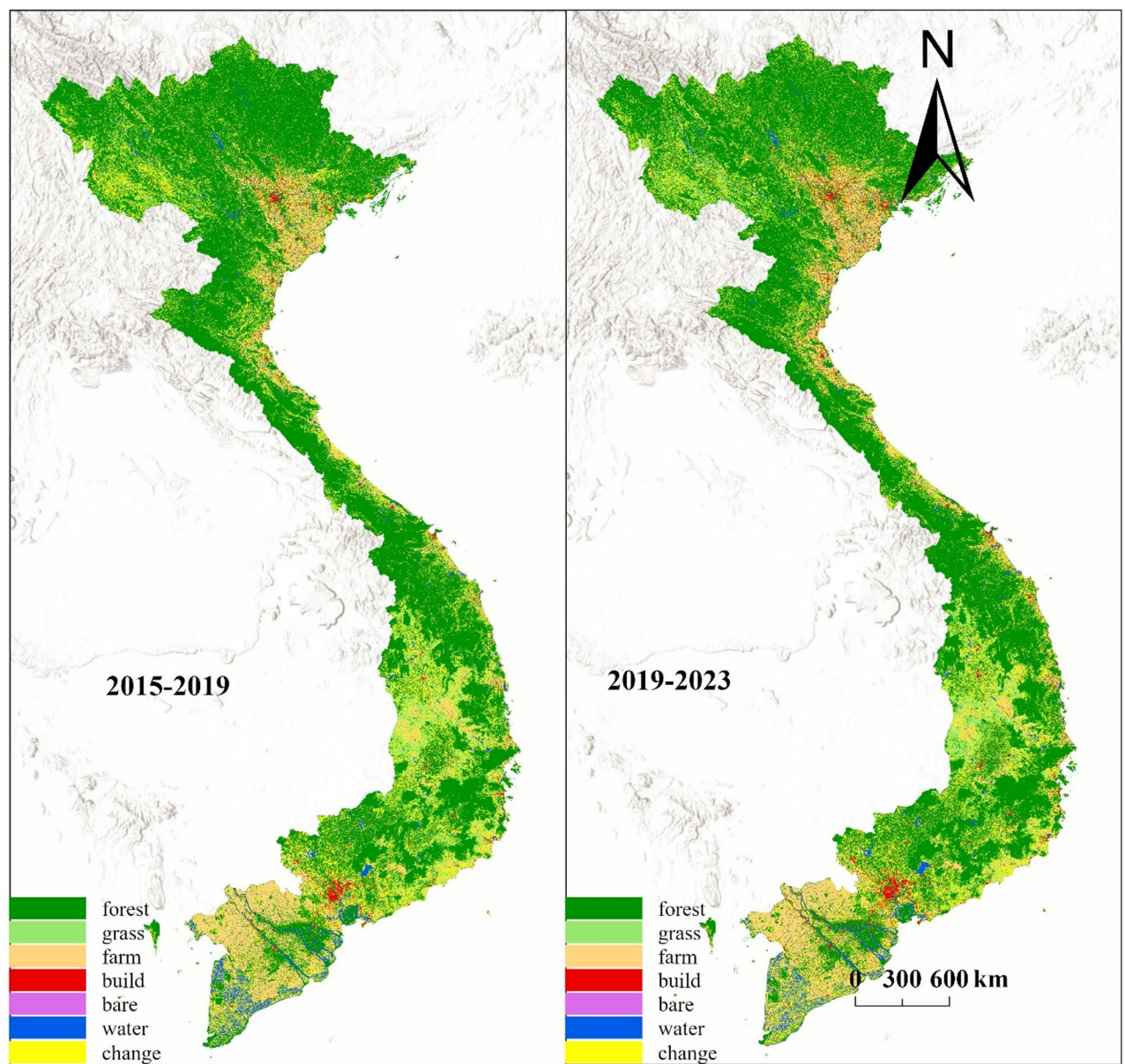


**Fig. 4.** LULC shift maps. This figure is generated using ArcGIS Pro 3.0.1 (<https://www.esri.com/zh-cn/arcgis/products/arcgis-pro/overview>) while the country boundary is extracted from the GADM (<https://gadm.org/>).

2015	2019					
Unit: (10 <sup>6</sup> m <sup>2</sup> )	Forest	Grassland	Farm	Build-up land	Bare land	Water bodies
Forest	1992.25	190.26	88.8	36.75	1.79	33.08
Grassland	80.72	153.03	28.98	9.38	0.84	1.1
Farm	74.5	50.1	314.83	3.03	0.59	17.87
Build-up land	17.8	7.14	2.23	48.75	0.25	0.36
Bare land	4.96	23.4	18.1	2.99	2.62	3.67
Water bodies	0.99	1.54	3.7	0.06	0.23	77.57

**Table 8.** Statistics on LULC changes from 2015 to 2019.

2019	2023					
Unit: (10 <sup>6</sup> m <sup>2</sup> )	Forest	Grassland	Farm	Build-up land	Bare land	Water bodies
Forest	1962.33	101.34	65.12	35.09	3.62	3.73
Grassland	163.57	198.11	41.11	13.95	5.95	2.76
Farm	59.43	38.34	336.75	5.18	10.36	6.58
Build-up land	12.66	3.03	0.84	81.35	2.69	0.37
Bare land	0.69	1.16	0.95	0.87	2.21	0.42
Water bodies	2.62	0.74	29.4	0.53	2.73	97.63

**Table 9.** Statistics on LULC changes from 2019 to 2023.

**Discussion**  
**Innovations and shortcomings of the classification method**

In this research, we employed the GEE platform alongside the random forest technique, analyzing the climatic features and growth patterns of rice. LULC and cover were comprehensively mapped across the entire territory of Vietnam with notable accuracy. Nevertheless, the approach of “classifying initially and comparing subsequently” that we chose might have missed the temporal continuity of LULC and cover types. This oversight could result in abrupt and substantial shifts in LULC types at varying times<sup>40–42</sup> potentially compromising the precision and reliability of the analysis concerning LULC change patterns in the area of study. Moreover, due to the time limitations of S2 imagery and the persistent cloud cover in northern Vietnam, the classification accuracy for 2015 and 2016 might be slightly lower; due to the limitations inherent in RF classification accuracy, this research did not differentiate between the types of forest land, such as natural, shrub, and economic forests; nor did it make distinctions among open water bodies and fisheries within aquatic categories, or between drylands and farmland in the agricultural classifications. This may render the land mapping findings of this study somewhat coarse and insufficiently detailed regarding the land classification system. Notably, this research enhanced the classification accuracy for various vegetation types and farmland within the region by incorporating regional sample points alongside the phenological characteristics of local vegetation. This indicates that integrating regional sample data and climatic factors into LULC classification proves effective and viable in enhancing classification accuracy.

**Causes, impacts, and driving mechanisms of LULC changes**

In this study, from 2015 to 2023, the area of forests and bare land in Vietnam decreased, and the area of constructed land, grassland, farmland, and water bodies increased to varying degrees. This finding is consistent with the findings of BB Thien et al. in Phu Tho Province, Vietnam<sup>43</sup> and Thi-Thu Vu et al. in Dong Dau District, Vietnam<sup>44</sup> who showed that land-use changes in Vietnam were mainly characterized by a decrease in the area of vegetation and bare land and an increase in the area of constructed land, grassland, farmland and water bodies. In the first five years, 8.12% of forests were converted to grassland and 3.79% to cropland. The large-scale conversion of forests to grassland may be attributed to the continuous expansion of human activity areas, which affected the forest ecosystem, leading to the degradation of primary forests into shrubland and grassland. Subsequently, some grassland suitable for agricultural production was further developed into cropland, resulting in the large-scale conversion of forests into grassland and cropland LULC types. In the following five years, the conversion areas decreased to 4.66% and 2.99%, respectively. This could be due to the implementation of Vietnam’s forest protection policies, which slowed the rate of forest area conversion. Meanwhile, the area of grassland converted to forests continued to increase, likely benefiting from the rapid development of the artificial forest economy supported by Vietnam’s policies, with large areas of grassland being converted into artificial forests.

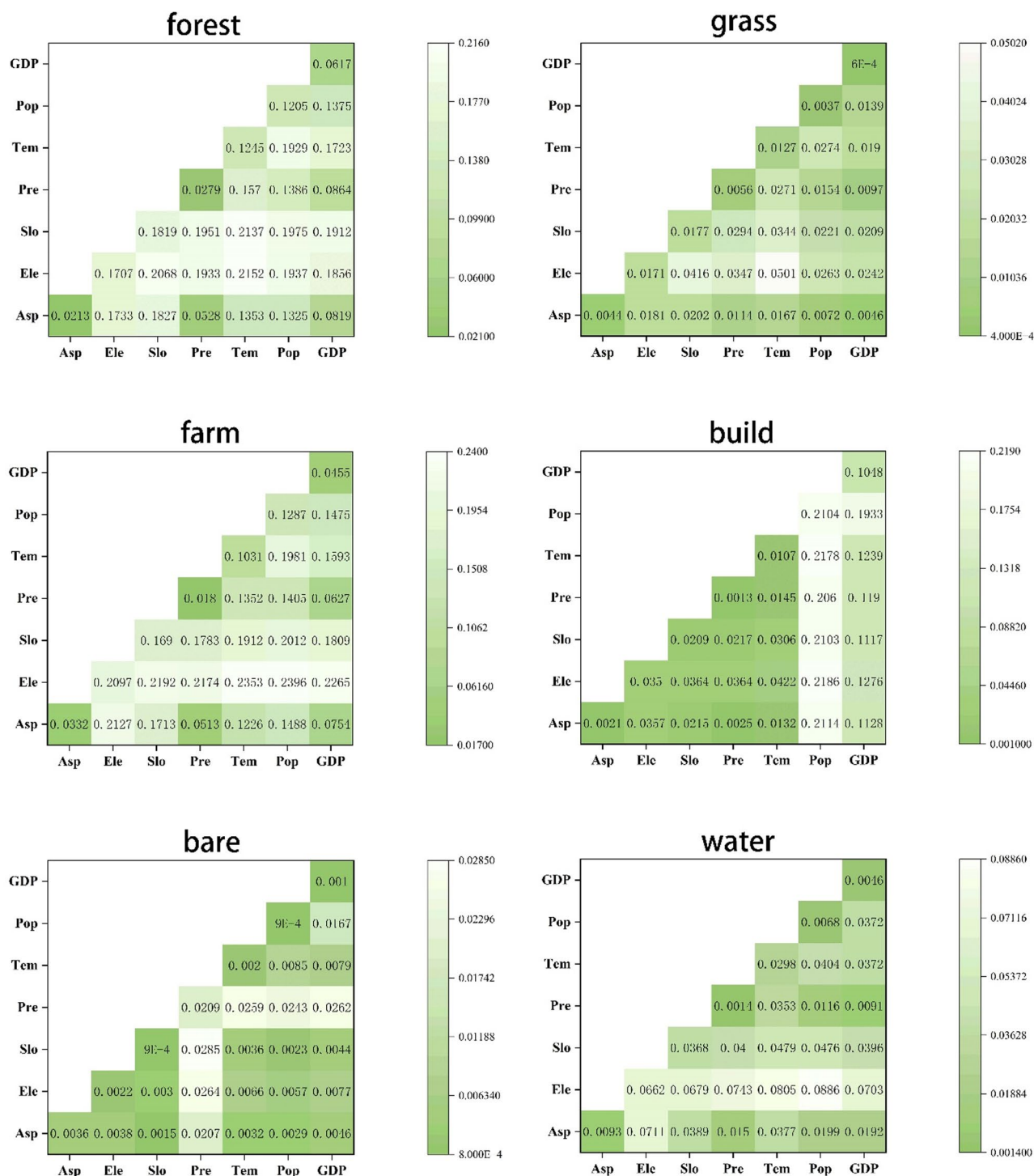
Over the past decade, this paper highlights that a significant portion of forests in Vietnam has been converted to grasslands, while a considerable amount of grasslands has been transformed into forested areas. Additionally, a majority of farmland and bare land has shifted into both forests and grasslands. These phenomena indicate that Vietnam’s forest conservation policies are beginning to bear fruit<sup>45</sup> and that Vietnam is one of the few “models of successful forest restoration” that have significantly increased forest cover as a result of government-led forest policies or initiatives<sup>46</sup>. Therefore, the Vietnamese government should advocate for the development of agricultural intensification to enhance food productivity without expanding farmland areas, continue to maintain existing land planning and management measures, further promote local sustainable development, and contribute to achieving regional carbon neutrality goals<sup>47</sup>.

This research indicates that LULC in Vietnam are impacted by a mix of socio-economic and climatic-environmental elements, particularly the significant factors of slope, elevation, temperature, and population. These findings align with earlier research conducted in the central region<sup>48</sup> as well as in the southern delta<sup>49</sup> of Vietnam. Additionally, the influence of precipitation on changes in LULC within Vietnam was found to be minimal, largely due to the country’s position within a tropical monsoon climate, where precipitation has historically not been a primary factor affecting the alterations in land surface ecosystems.

**Carbon stock changes and analysis**

Between 2015 and 2023, Vietnam’s total carbon storage showed a trend of continuous decline initially, followed by a fluctuating increase. However, it did not reach the carbon storage levels of 2015. Forest carbon stock generally declined during this period, which is related to the reduction of forest area due to land development

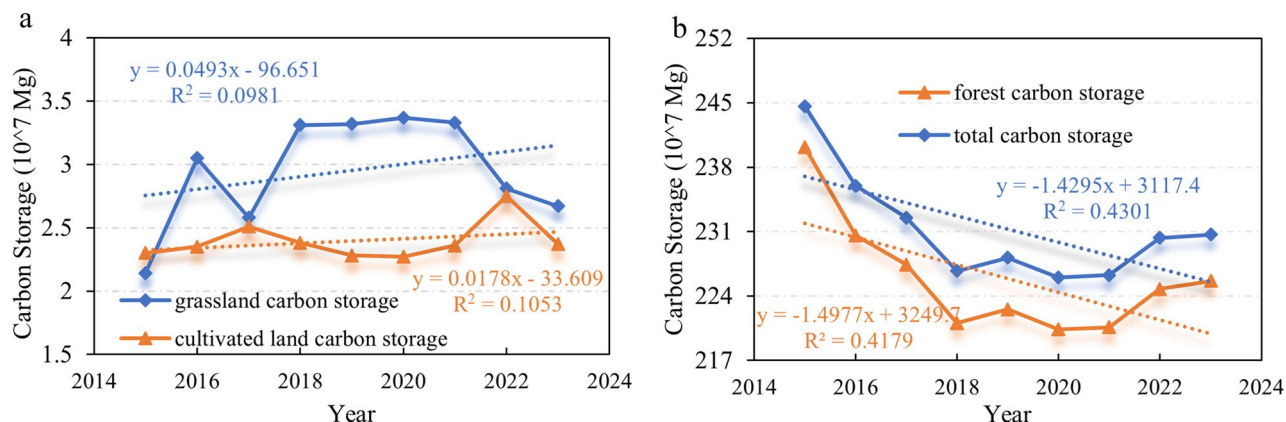




**Fig. 5.** Heat map of driving factor interaction effects. Asp, Ele, Slo, Pre, Tem, Pop division representative aspect, elevation, slope, precipitation, temperature and population.

and deforestation. The carbon storage in grasslands and croplands fluctuated, but their impact on total carbon storage was relatively small. The areas with significant differences in carbon storage distribution are primarily located at the boundaries between forests and agricultural or urban land, as well as at the interfaces between mountainous and plain terrains. These variations are mainly influenced by a combination of human activities and topographical factors. In the future, forest protection and ecological restoration need to be strengthened in order to effectively increase carbon stocks and achieve sustainable development.

LULC type( $\times 10^7$ Mg C)	2015	2016	2017	2018	2019	2020	2021	2022	2023
Forest carbon storage	240.15	230.58	227.42	221.03	222.55	220.4	220.59	224.75	225.63
Grassland carbon storage	2.14	3.05	2.58	3.31	3.32	3.37	3.33	2.81	2.67
Farmland carbon storage	2.3	2.35	2.51	2.38	2.28	2.27	2.36	2.75	2.37
Total carbon storage	244.59	235.98	232.5	226.72	228.15	226.04	226.28	230.31	230.68

**Table 10.** Vietnam's annual carbon storage statistics.**Fig. 6.** Vietnam continuous carbon storage change maps.

## Conclusion

Being the second largest exporter of rice globally and a significant recipient of industrial transfers from China, Vietnam faces challenges such as the unavailability of high-precision, automated LULC classification data on a national scale, a dearth of research focused on technologies driven by LULC changes, and insufficient statistics for assessing the national carbon stock of Vietnam. This research utilizes the GEE platform, leveraging data from both S1 and S2 satellites. We employed the “Multi-source Consistency,” “Time Series Stability,” and Random Forest methodologies to produce high-precision LULC datasets for Vietnam covering the years 2015–2020. The technical strategies and modeling techniques implemented in this paper have markedly enhanced the classification accuracy of different LULC categories, as well as the precision in identifying farmland, providing valuable reference data for comparable studies in other regions in the future. The findings indicate that in Vietnam, forested areas are the predominant LULC type, with a notable reduction in forested regions since 2015. Additionally, grasslands and water bodies exhibited variability, while there has been a steady increase in the extent of urbanized land, no substantial change in farmland areas, and a gradual decline in bare land. Through Geo-Detector, we found that the change of area of forest and farmland is mainly affected by slope, elevation and population, the area of construction land is mainly affected by population and GDP, and the influencing factors of grassland, bare land and water bodies do not obviously manifest themselves in a specific category. Through the analysis we found that agricultural expansion and urbanization are the main reasons for the disappearance of forests. Whereas the increase in grassland area is mainly attributed to the conversion of forests and farmland, especially the high percentage of conversion from farmland to grassland, while the area of farmland shows a trend of increasing and then decreasing. As of 2023, Vietnam's carbon stock has  $230.68 \times 10^7$  Mg C. the overall carbon stock shows a slow downward trend from  $244.59 \times 10^7$  Mg C in 2015 to a low of  $226.04 \times 10^7$  Mg C in 2020, and then gradually rebounds to  $230.68 \times 10^7$  Mg C in 2023. among them, forests account for the largest share of the carbon stock and the overall trend is decreasing and the distribution of carbon stocks shows obvious geographical differences. The carbon stock is high in the north and center of Vietnam, and low in the Mekong and Red River deltas. In the future, it is necessary to maintain and strengthen ecological protection in order to effectively increase carbon stocks and achieve the goal of carbon neutrality in the region.

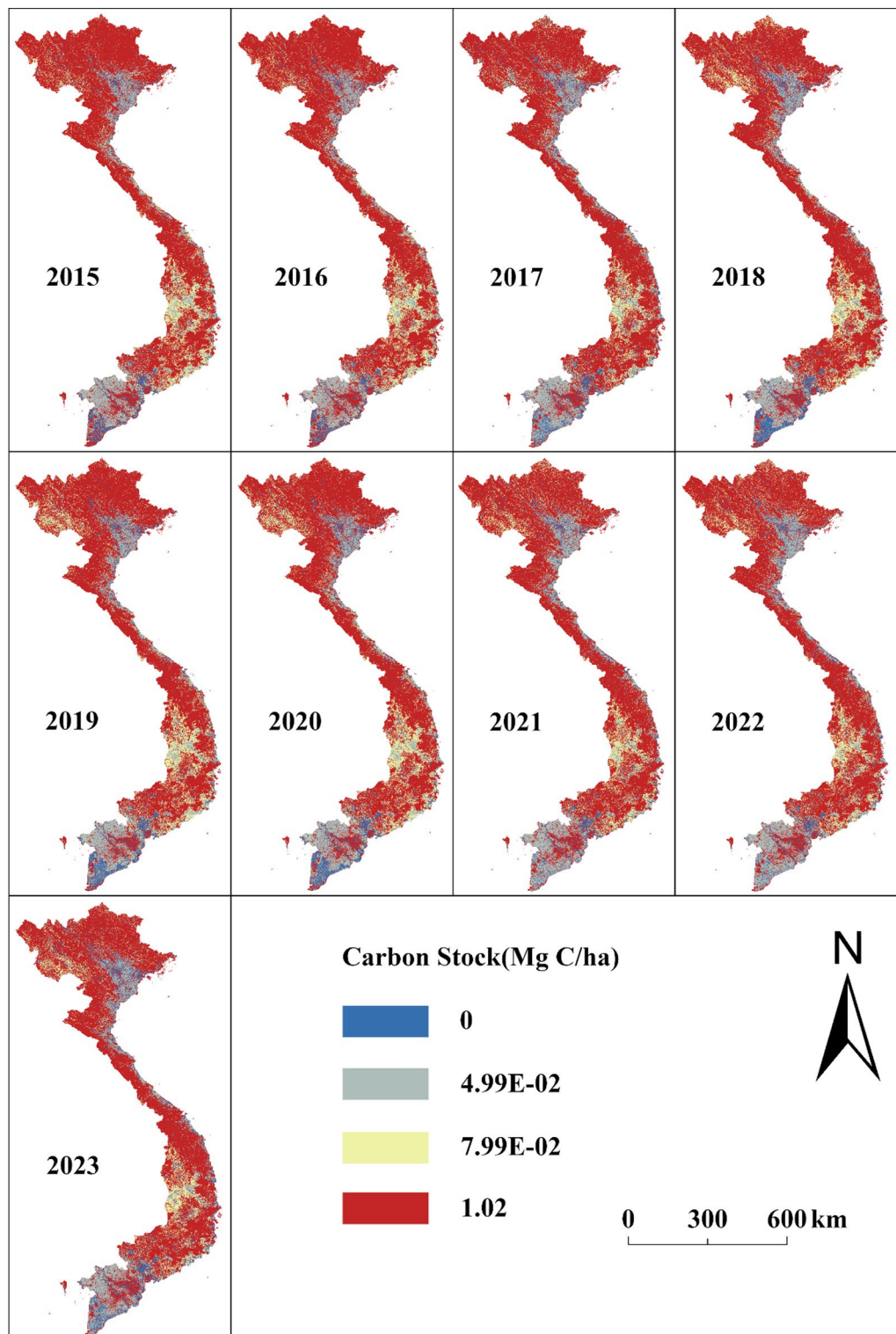


**Fig. 7.** Multi-year carbon storage maps. This figure is generated using ArcGIS Pro 3.0.1 (<https://www.esri.com/zh-cn/arcgis/products/arcgis-pro/overview>) while the country boundary is extracted from the GADM (<https://gadm.org/>).

## Data availability

The datasets used and or analyzed in this study are available from the corresponding author on reasonable request.

Received: 6 September 2024; Accepted: 28 May 2025

Published online: 01 July 2025

## References

1. Su, J., Teng, H.H., Wan, X., Zhang, J., Liu, C.Q. Direct air capture of CO<sub>2</sub> through carbonate alkalinity generated by phytoplankton nitrate assimilation. *Int. J. Environ. Res. Public Health* **20**, (2022).
2. Winkler, K., Fuchs, R., Rounsevell, M. & Herold, M. Global land use changes are four times greater than previously estimated. *Nat. Commun.* **12**, 2501 (2021).
3. Qin, Z. et al. Global spatially explicit carbon emissions from land-use change over the past six decades (1961–2020). *One Earth* **7**, 835–847 (2024).
4. Lambin, E. F., Geist, H. J. & Lepers, E. Dynamics of land-use and land-cover change in tropical regions. *Ann. Rev. Environ. Resour.* **28**, 205–241 (2003).
5. Xiang, M. et al. Spatio-temporal evolution and driving factors of carbon storage in the Western Sichuan Plateau. *Sci. Rep.* **12**, 8114 (2022).
6. Liu, J., Yan, Q. & Zhang, M. Ecosystem carbon storage considering combined environmental and land-use changes in the future and pathways to carbon neutrality in developed regions. *Sci. Total Environ.* **903**, 166204 (2023).
7. Chen, L. et al. Strategies to achieve a carbon neutral society: a review. *Environ. Chem. Lett.* **20**, 2277–2310 (2022).
8. Chuai, X. et al. Promoting low-carbon land use: from theory to practical application through exploring new methods. *Human. Soc. Sci. Commun.* **11**, 727 (2024).
9. Sha, Z. et al. The global carbon sink potential of terrestrial vegetation can be increased substantially by optimal land management. *Commun. Earth Environ.* **3**, 8 (2022).
10. Marques, A. et al. Increasing impacts of land use on biodiversity and carbon sequestration driven by population and economic growth. *Nat. Ecol. Evol.* **3**, 628–637 (2019).
11. Zhang, L. et al. Conversion of farmland to forest or grassland improves soil carbon, nitrogen, and ecosystem multi-functionality in a subtropical karst region of southwest China. *Sci. Rep.* **14**, 17745 (2024).
12. Song, X.-P. et al. Global land change from 1982 to 2016. *Nature* **560**, 639–643 (2018).
13. Aryal, J., Sitaula, C. & Frery, A. C. Land use and land cover (LULC) performance modeling using machine learning algorithms: a case study of the city of Melbourne, Australia. *Sci. Rep.* **13**, 13510 (2023).
14. Zhang, G., Roslan, S. N. A., Wang, C. & Quan, L. Research on land cover classification of multi-source remote sensing data based on improved U-net network. *Sci. Reports* **13**, 16275 (2023).
15. Shafizadeh-Moghadam, H., Khazaei, M., Alavipanah, S. K. & Weng, Q. Google Earth Engine for large-scale land use and land cover mapping: an object-based classification approach using spectral, textural and topographical factors. *GIScience Remote Sens.* **58**, 914–928 (2021).
16. Yan, J. et al. A time-series classification approach based on change detection for rapid land cover mapping. *ISPRS J. Photogramm. Remote Sens.* **158**, 249–262 (2019).
17. Campos-Taberner, M. et al. Understanding deep learning in land use classification based on Sentinel-2 time series. *Sci. Reports* **10**, 17188 (2020).
18. Amani, M. et al. Google earth engine cloud computing platform for remote sensing big data applications: a comprehensive review. *IEEE J. Select. Top. Appl. Earth Observ. Remote Sens.* **13**, 5326–5350 (2020).
19. Tamiminia, H. et al. Google Earth Engine for geo-big data applications: a meta-analysis and systematic review. *ISPRS J. Photogramm. Remote Sens.* **164**, 152–170 (2020).
20. Amani, M. et al. A generalized supervised classification scheme to produce provincial wetland inventory maps: an application of Google Earth Engine for big geo data processing. *Big Earth Data* **3**, 378–394 (2019).
21. Li, M. et al. Application of geographical detector and geographically weighted regression for assessing landscape ecological risk in the Irtys River Basin, Central Asia. *Ecol. Indicators* **158**, 111540 (2024).
22. Li, R., Ye, C., Wang, Y., Han, G. & Sun, J. Carbon storage estimation and its driving force analysis based on InVEST model in the Tibetan Plateau. *Acta Agrestia Sinica* **29**, 43 (2021).
23. Zhao, K. et al. Utility of multitemporal lidar for forest and carbon monitoring: tree growth, biomass dynamics, and carbon flux. *Remote Sens. Environ.* **204**, 883–897 (2018).
24. Kelong, C. et al. The study of vegetation carbon storage in Qinghai Lake Valley based on remote sensing and CASA model. *Procedia Environ. Sci.* **10**, 1568–1574 (2011).
25. Andersen, L. E. et al. Net Carbon Emissions from Deforestation in Bolivia during 1990–2000 and 2000–2010: results from a carbon bookkeeping model. *PLoS ONE* **11**, e0151241 (2016).
26. Zhao, M. et al. Assessing the effects of ecological engineering on carbon storage by linking the CA-Markov and InVEST models. *Ecol. Indicators* **98**, 29–38 (2019).
27. Babbar, D. et al. Assessment and prediction of carbon sequestration using Markov chain and InVEST model in Sariska Tiger Reserve, India. *J. Clean. Prod.* **278**, 123333 (2021).
28. Yang, J., Xie, B. & Zhang, D. Spatio-temporal evolution of carbon stocks in the Yellow River Basin based on InVEST and CA-Markov models. *Chin. J. Eco-Agric.* **29**, 1018–1029 (2021).
29. Adellisardou, F. et al. Spatiotemporal change detection of carbon storage and sequestration in an arid ecosystem by integrating Google Earth Engine and InVEST (the Jiroft plain, Iran). *Int. J. Environ. Sci. Technol.* **1**–16 (2022).
30. Bui, T. H. H. & Chen, Q. An analysis of factors influencing rice export in Vietnam based on gravity model. *J. Knowl. Econ.* **8**, 830–844 (2017).
31. Jia, K. et al. Land cover classification of Landsat data with phenological features extracted from time series MODIS NDVI data. *Remote Sens.* **6**, 11518–11532 (2014).
32. Niu, X. et al. Temporal and spatial evolution characteristics and its driving mechanism of land use/cover in Vietnam from 2000 to 2020. *Land* **11**, 920 (2022).
33. Guo, X., Ye, J. & Hu, Y. Analysis of land use change and driving mechanisms in Vietnam during the period 2000–2020. *Remote Sens.* **14**, 1600 (2022).
34. Mullissa, A. et al. Sentinel-1 sar backscatter analysis ready data preparation in google earth engine. *Remote Sens.* **13**, 1954 (2021).
35. Rumora, L., Miler, M. & Medak, D. Impact of various atmospheric corrections on sentinel-2 land cover classification accuracy using machine learning classifiers. *ISPRS Int. J. Geo-Inf.* **9**, 277 (2020).
36. Phiri, D. et al. Sentinel-2 data for land cover/use mapping: a review. *Remote Sens.* **12**, 2291 (2020).
37. Skriver, H. et al. Crop classification using short-revisit multitemporal SAR data. *IEEE J. Select. Topic Appl. Earth Observ. Remote Sens.* **4**, 423–431 (2011).



38. Shaik, A. B., Srinivasan, S. in *International Conference on Innovative Computing and Communications: Proceedings of ICICC 2018, Volume 2*. (Springer, 2019), pp. 253–260.
39. Wang, J. F. et al. Geographical detectors-based health risk assessment and its application in the neural tube defects study of the Heshun Region, China. *Int. J. Geogr. Inf. Sci.* **24**, 107–127 (2010).
40. Ye, J., Hu, Y., Zhen, L., Wang, H. & Zhang, Y. Analysis on Land-Use Change and its driving mechanism in Xilingol, China, during 2000–2020 using the google earth engine. *Remote Sens.* **13**, 5134 (2021).
41. Hu, Y. & Hu, Y. Land cover changes and their driving mechanisms in Central Asia from 2001 to 2017 supported by Google Earth Engine. *Remote Sens.* **11**, 554 (2019).
42. Kennedy, R. E., Yang, Z. & Cohen, W. B. Detecting trends in forest disturbance and recovery using yearly Landsat time series: 1. LandTrendr—Temporal segmentation algorithms. *Remote Sens. Environ.* **114**, 2897–2910 (2010).
43. Thien, B. B. & Phuong, V. T. Analyzing and modeling land use/land cover change in Phu Tho Province, Vietnam. *J. Degrad. Min. Lands Manag.* **11**, 5225–5235 (2024).
44. Vu, T.-T. & Shen, Y. Land-use and land-cover changes in dong Trieu district, Vietnam, during past two decades and their driving forces. *Land* **10**, 798 (2021).
45. Dang, T. K. P. The discourse of forest cover in Vietnam and its policy implications. *Sustainability* **14**, 10976 (2022).
46. MacDicken, K. G. Management, Global forest resources assessment 2015: what, why and how?. *Forest Ecol. Manag.* **352**, 3–8 (2015).
47. Hauser, L. T., An Binh, N., Viet Hoa, P., Hong Quan, N. & Timmermans, J. Gap-free monitoring of annual mangrove forest dynamics in ca mau province, vietnamese mekong delta, using the landsat-7–8 archives and post-classification temporal optimization. *Remote Sens.* **12**, 3729 (2020).
48. Disperati, L. & Virdis, S. G. P. Assessment of land-use and land-cover changes from 1965 to 2014 in Tam Giang-Cau Hai Lagoon, Central Vietnam. *Appl. Geogr.* **58**, 48–64 (2015).
49. Minderhoud, P. et al. The relation between land use and subsidence in the Vietnamese Mekong delta. *Sci. Total Environ.* **634**, 715–726 (2018).

## Author contributions

Y.L. analyzed data and wrote this manuscript. K.Y. conceived the idea, reviewed this manuscript and provided technical guidance. Z.Q.P. Writing-Reviewing and Editing, Project Administration. T.L.Z. helped in simulations and improved the grammar and comprehension. D.N.S. and R.S. helped in interpreting the results and proof read the draft. J.C.M. provided critical feedback in finalizing this draft.

## Funding

This research was supported by National Natural Science Foundation of China (Grants Nos. 42071381).

## Declarations

## Competing interests

The authors declare no competing interests.

## Software and tools

The following software and packages were used for data processing and analysis in this study: Google Earth Engine (GEE) – Utilized for Sentinel image acquisition, preprocessing, and classification. Version: Latest online version. URL: <https://earthengine.google.com/>. ArcGIS Pro – Applied for spatial analysis and visualization. Version: 3.0.1. URL: <https://www.esri.com/en-us/arcgis/products/arcgis-pro/overview>. InVEST – Employed for carbon stock estimation and the generation of carbon stock maps. Version: 3.14.1. URL: <https://naturalcapitalproject.stanford.edu/software/invest>. R – Used for the statistical analysis of driving factors. Version: 4.4.0. URL: <https://cran.r-project.org/>.

## Additional information

**Correspondence** and requests for materials should be addressed to K.Y. or Z.P.

**Reprints and permissions information** is available at [www.nature.com/reprints](http://www.nature.com/reprints).

**Publisher's note** Springer Nature remains neutral with regard to jurisdictional claims in published maps and institutional affiliations.

**Open Access** This article is licensed under a Creative Commons Attribution-NonCommercial-NoDerivatives 4.0 International License, which permits any non-commercial use, sharing, distribution and reproduction in any medium or format, as long as you give appropriate credit to the original author(s) and the source, provide a link to the Creative Commons licence, and indicate if you modified the licensed material. You do not have permission under this licence to share adapted material derived from this article or parts of it. The images or other third party material in this article are included in the article's Creative Commons licence, unless indicated otherwise in a credit line to the material. If material is not included in the article's Creative Commons licence and your intended use is not permitted by statutory regulation or exceeds the permitted use, you will need to obtain permission directly from the copyright holder. To view a copy of this licence, visit <http://creativecommons.org/licenses/by-nc-nd/4.0/>.

© The Author(s) 2025